HIGHLY SENSITIVE AIRBORNE OPEN PATH OPTICAL HYGROMETER FOR UPPER AIR MEASUREMENTS – PROOF OF CONCEPT

Tadeusz Stacewicz[1], Paweł Magryta[1], Bendix Petersen[2], Jakub L. Nowak[3], Kamil Kwiatkowski[4], Szymon P. Malinowski[3]

1) *University of Warsaw, Faculty of Physics, Pasteura 5, 02-093 Warsaw, Poland (✉ tadstac@fuw.edu.pl, +48 22 553 743, pawel.magryta@fuw.edu.pl)*

2) *Humboldt-Universität zu Berlin, Department of Physics, Newtonstraße 15, 12489 Berlin, Germany (idir@physik.hu-berlin.de)*

3) *University of Warsaw, Faculty of Physics, 02-093 Warsaw, Pasteura 7, Poland (jakub.nowak@fuw.edu.pl, malina@fuw.edu.pl)*

4) *University of Warsaw, Interdisciplinary Centre for Mathematical and Computational Modelling, Pawinskiego 5a, 02-106 Warsaw, Poland (kamil.kwiatkowski@fuw.edu.pl)*

Abstract

A concept of a highly sensitive and fast-response airborne optoelectronic hygrometer, based on the absorption spectroscopy with laser light tuned to an intense ro-vibronic absorption line of H_2O in the 1391–1393 nm range is presented. The target application of this study is airborne atmospheric measurements, in particular at the top of troposphere and in stratosphere. The cavity ring-down spectroscopy was used to achieve high sensitivity. In order to avoid interference of the results by water desorbed from the instrument walls, the open-path solution was applied. Tests of the instrument, performed in a climatic chamber, have shown some advantages of this concept over typical hygrometers designed for similar applications.

Keywords: humidity, hygrometer, laser, absorption, CRDS.

1. Introduction

Highly sensitive and fast-response measurements of H_2O concentration in gases are widely used in various fields, from the technological ones to geophysical research. In-situ humidity measurements are of great significance in atmospheric physics. Water vapour is the most important greenhouse gas absorbing the energy irradiated from the Earth surface. It is involved in climate feedback loops that include complicated interactions between water vapour, clouds, atmospheric circulations, convection and radiation [1, 2]. Moreover, the monitoring of long-term changes in water vapour, which are closely linked to other climate variations and trends, is needed to both prediction and detection of the changes as well as for testing theoretical models [3].

Water is a substance poorly mixed in the atmosphere. The mean quantity of H_2O molecules exceeds about 10^{17} cm^{-3} at low altitudes, but it decreases below 10^{12} cm^{-3} at an altitude of 40 km (Fig. 1). Nevertheless, local H_2O concentrations in atmosphere might change even by

several orders of magnitude in neighbouring regions within a scale of hundred metres or less, due to turbulent mixing with air particles or masses of different history.

In particular, the detailed information on sub/supersaturation in reference to water and ice is crucial to understanding life cycles of cirrus clouds [4] and stratosphere dehydration [5]. Other important processes include mixing and transport across tropopause due to gravity waves over-shooting cumulonimbus tops. Thus, having an opportunity of accurate and high-resolution measurements of H_2O concentration in various conditions is very important.

Airborne measurements of humidity are important tools to provide basic in-situ information on water vapour concentration. The results of such measurements are used for validation and verification of remote measurements [6, 7]. They are also applied to testing and verification of numerical weather prediction models, simulations of pollution transport or radiative transfer models. However, airborne measurements of H_2O molecules' concentration in the Earth's atmosphere are challenging not only because of a wide range of the observed values (exceeding 5 orders of magnitude, Fig. 1), but also due to a high span of environmental conditions: temperature and pressure in which the measurements have to be taken. Phase changes and the existence of water in various forms (from gas or liquid drops and droplets to solid ice crystals), complicated transport phenomena due to advection, convection, turbulence, sedimentation, precipitation, result in a high variability of humidity in all scales.
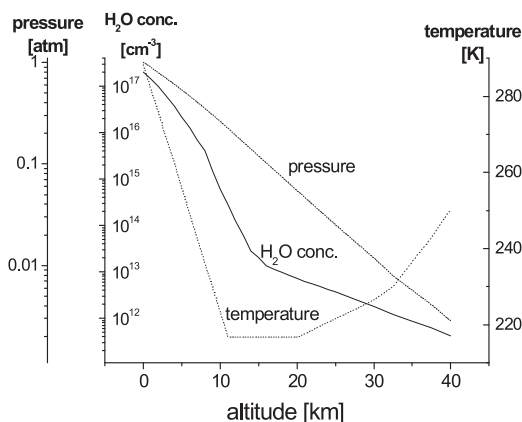

Fig. 1. Distributions of pressure, temperature and H_2O concentration in atmosphere (the standard US model [8]).

A variety of hygrometers are used in airborne measurements (see *e.g.* Subsection 2.6 in [9]). They include fast-response optical hygrometers, highly accurate dew point meters, psychrometers, thin-film capacitance meters and many others [10, 11]. Optical airborne hygrometers based on the wavelength modulation spectroscopy with a detection limit of $3.6 \cdot 10^{11}$ cm^{-3} were demonstrated by Zondlo *et al.* [12]. Other airborne tuneable diode laser hygrometers were described by Buchholz *et al.* [13, 14] and Sonnenfroh *et al.* [15]. A fast-response optical hygrometer with the reaction time shorter than 10^{-2} s was presented by Nowak *et al.* [16]. In the study presented in this paper we focus on optical sensors aimed at the detection of water vapour concentration based on measurement of the radiation absorption in a near-infrared range. Hygrometers based on CRDS approach with a sensitivity of about 1 nmol/mol were already demonstrated by Abe and Yamada [17]. In the already mentioned work such devices are used in the airborne applications, but in a close-path design [12].

2. Principles of measurement

The concept of our hygrometer is based on the absorption spectroscopy of light tuned to an intense ro-vibronic line of H_2O molecule. An ultrasensitive laser spectroscopy (CRDS) setup with an open light path was applied. This technique ensures high sensitivity of the instrument while it is suitable for detection of weak absorption [18, 19]. In such a configuration relatively fast and sensitive measurements are available.

2.1. Cavity Ring-Down Spectroscopy

The absorption coefficient is usually determined with CRDS due to measurement of a photon lifetime in the cavity [19]. The lifetime is measured once for the cavity without an absorber (τ_0) and then for the case when the resonator is filled with the investigated gas (τ). The absorber concentration is found from the formula:

$$N = \frac{1}{\sigma c}\left(\frac{1}{\tau} - \frac{1}{\tau_0}\right),\tag{1}$$

where c denotes the light speed and σ is the absorption cross-section. However, for an AM-modulated light beam illuminating the cavity the harmonics of the output signals are delayed in reference to the relevant harmonics or the input signals [20]. Then, a phase shift occurs due to the energy stored in the cavity. For the n-th harmonic of modulation frequency f such a phase shift φ_n fulfils the relation:

$$\tan\varphi_n = -2\pi n f \tau.\tag{2}$$

The phase shift can be measured with a lock-in voltmeter for both cases: the empty cavity (φ_{n0}) and the cavity filled with an absorber (φ_n). Combining the equations (1) and (2) one can find another formula for the absorber concentration:

$$N = \frac{2\pi n f}{\sigma c}\left(\cot\varphi_{n0} - \cot\varphi_n\right).\tag{3}$$

Due to a high capability of lock-in detection to improve the signal to noise ratio, the phase shift can be determined with a good precision (~ 0.006 rad). Therefore, this approach was used in our system.

2.2. Wavelength selection

The sensitive optical hygrometry requires selecting a molecular spectral band with a large absorption cross-section. The absorption spectrum of H_2O consists of 5 bands in the NIR – MIR range. The highest values of cross-section can be found around 5930 nm. However, constructing a sensor based on these transitions would be relatively complicated due to a necessity of using specialized optical materials as well as expensive quantum cascade lasers. Moreover, a relatively low sensitivity of the MIR photodetectors brings serious problems for the application of CRDS. The next band, located in shorter wavelengths (around 2670 nm), includes the lines of comparable cross-sections. While common optic materials and diode lasers might be applied in this range, a suitable fibre equipment (couplers, modulators, *etc.*) is still under development and requires an improvement in comparison with a wide choice of such devices at shorter wavelengths. From this point of view the 1350–1420 nm absorption band is much more convenient, since the diode lasers, photodetectors and fibre optic instruments operating in this range are easily available and

www.czasopisma.pan.pl PAN www.journals.pan.pl
T. Stacewicz, P. Magryta, et al.: HIGHLY SENSITIVE AIRBORNE OPEN PATH OPTICAL...
POLSKA AKADEMIA NAUK

relatively inexpensive. Therefore, the lines from the 1391.5–1393.0 nm range were selected for our experiment.

2.3. Dependence of absorption spectrum on atmospheric conditions

The shapes of spectral lines in dense gases are mainly determined by collisions among molecules. In rough approximation the line profiles can be described by Voigt functions, however their precise determination is still a matter of intensive investigation [21, 22]. The line parameters are collected in databases, such as HITRAN [8].

The 1391.5–1393.0 nm absorption band that was used in our experiment is presented in Fig. 2 (in normal conditions). It consists of several lines characterized by various peak cross-sections. To achieve the best sensitivity of the hygrometer the strongest line (1392.5335 nm) was selected.
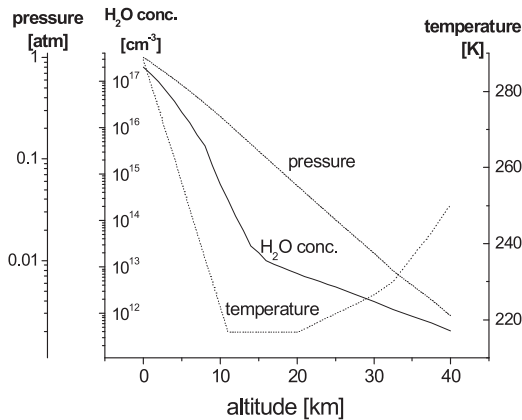

Fig. 2. An absorption spectrum of H_2O at around 1392 nm in normal conditions.

The shape of the absorption spectrum and its parameters, like the maximal cross-sections of the lines, their peak wavelengths as well as the widths, vary with changes of pressure, temperature and humidity. The pressure dependences are the strongest while the temperature influence is softer within the values occurring in atmosphere. Examples of these dependences for the H2O line used in our experiment (1392.5335 nm) are shown in Fig. 3.

Changes of H_2O line-shapes dependent on humidity are also observed (Fig. 3c). This effect, called self-broadening, becomes important at a high water vapour load. A decrease of the cross-section by about 1% (and a similar linewidth increase) is observed when the water concentration in atmosphere exceeds $5 \cdot 10^{16}$ cm^{-3} (Fig. 3c). No important impact on the peak line wavelength occurs due to humidity.

The experimental determination of the absorption coefficient α_λ in certain conditions and knowledge of the cross-section σ_λ enable to determine the water vapour concentration (N):

$$N_{H_2O} = \frac{\alpha_\lambda \left(p, T, N_{H_2O} \right)}{\sigma_\lambda \left(p, T, N_{H_2O} \right)}. \tag{4}$$

The dependences of pressure (p), temperature (T) and humidity (N_{H_2O}) on the H_2O spectrum force a proper arrangement of the optical detection experiment: these parameters must be
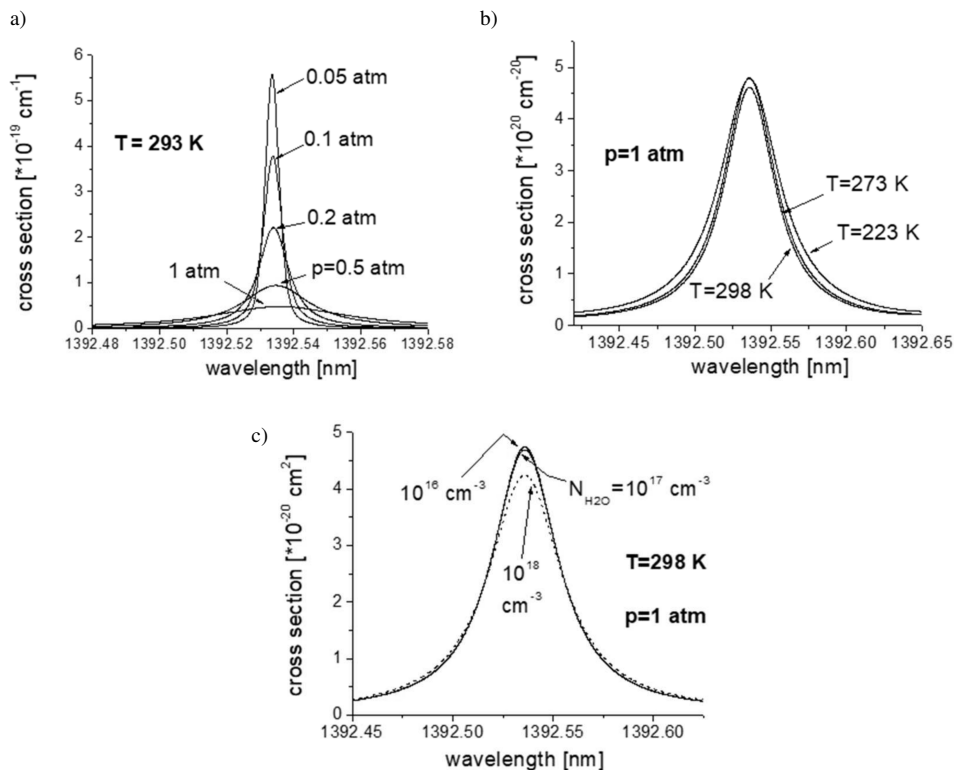
Fig. 3. Shapes of the 1392,5355 nm H_2O absorption line at various: a) air pressure; b) temperature; c) H_2O concentration.

measured simultaneously with the absorption coefficient. Their influence on the absorption cross-section must be taken into account in final data processing, according to (5). This aspect is very important, for instance – in the case of airborne application, in conditions strongly varying with altitude.

A typical FWHM width of the lines is equal to approximately $\Delta\lambda = 0.02-0.05$ nm in standard conditions; it decreases to a value close to its Doppler width (~ 0.0036 nm) at the altitude of 40 km (Fig. 4b). Simple analysis of the line shape shows that in order to measure the H_2O concentration with a precision better than $\pm 5\%$ one has to use a laser which wavelength is tuned to the peak of a selected line with a precision better than $\pm\Delta\lambda/3$. Also, the laser line width and the instability should be smaller than this value.

The wavelengths corresponding to the peaks of the spectral lines can change within the pressure range considered in this paper by about 0.05 nm. The line peak shift can occur due to a collisional disturbance of the molecular transition, but also due to the influence of the wings of neighbouring lines. These wings build up with the pressure rise. That can shift the position of the peaks lying on them: towards longer values when the peak is located on the long wavelength side of the disturbing line, and towards shorter wavelengths in the opposite case. The final line shift and the change of the corresponding cross-section are combinations of these effects which depend on many factors. They should be recognized for each line individually (see the examples in Fig. 4). Therefore, a precise laser tuning to the line peak and the following changes according
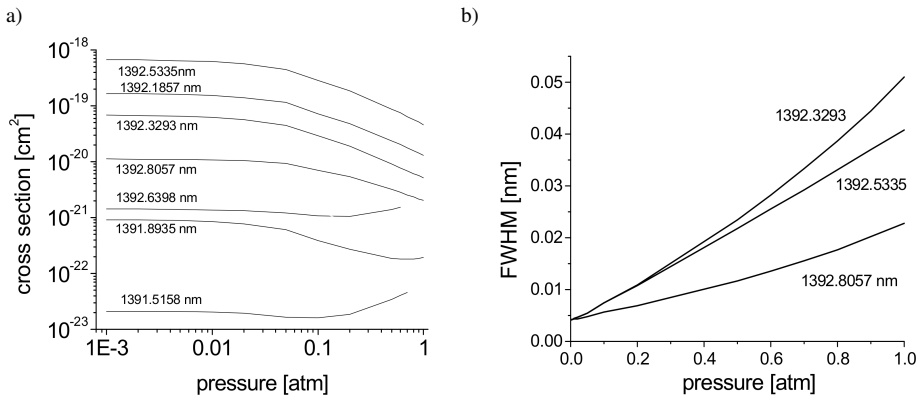
a)

b)

Fig. 4. The dependences on pressure of: a) a peak cross-section; b) a profile half-width for several lines
of the 1392 nm band.

to the variations of surrounding parameters should be performed [23]. That can be ensured by a careful laser wavelength control with a wave-meter or a system using a reference cell with H_2O vapour [16].

2.4. Influence of other absorbing gases

The next important aspect in optical water detection is its sensitivity to interferences of different compounds of atmosphere. Carbon dioxide and methane are the main interference sources. Their mean concentrations depending on altitude and the absorption spectra are presented in Fig. 5. The CO_2 concentration dominates over the H_2O load for altitudes higher than 10 km (Fig. 5a); above 15 km its density is larger than that of H_2O by about 2 orders of magnitude. Nevertheless, the carbon dioxide absorption cross-section (Fig. 5b) is 4–6 orders of magnitude smaller than that of H_2O, so – according to (4) – its disturbance of water vapour absorption is negligible within the wavelength range of 1391–1393 nm. The mean CH_4 concentration is smaller than the H_2O density at all altitudes. Taking into account that the absorption cross-section of
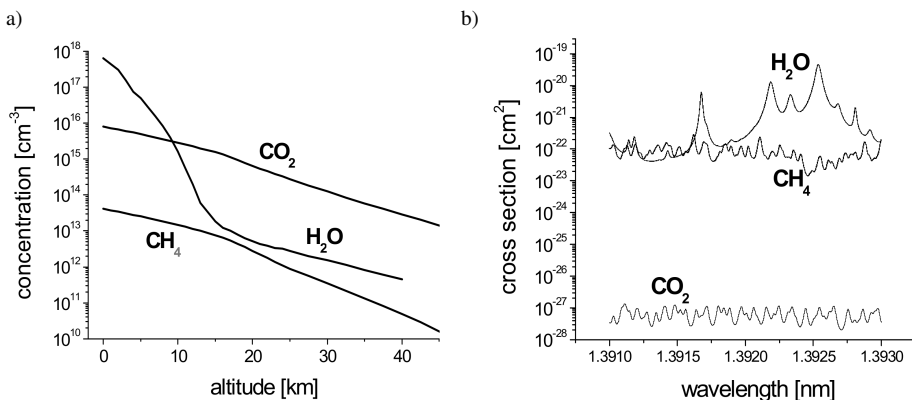
a)

b)

Fig. 5. a) Comparison of H_2O, CO_2 and CH_4 concentrations at various altitudes; b) absorption cross-sections
of these compounds in reference to H_2O in normal conditions.

methane is also about 1–2 orders of magnitude weaker within the 1392–1393 nm range, one can state that the disturbance of our hygrometer by this compound is also negligible.

3. Instrument

3.1. System design

The construction of our optical hygrometer is presented in Fig. 6. A single-mode 20 mW continuous wave diode laser (Toptica, DL 100), tuneable within the 1390–1395 nm range was used as the light source. The laser output was attached to the 10/90% fibre coupler. The out-coupled low-intensity part of the radiation was sent to the wavelength meter (High Precision, WS6 – 200) controlling the wavelength. The feedback from this instrument drove the laser current supply unit ensuring the wavelength tuning and stabilization with a precision of ± 0.001 nm.
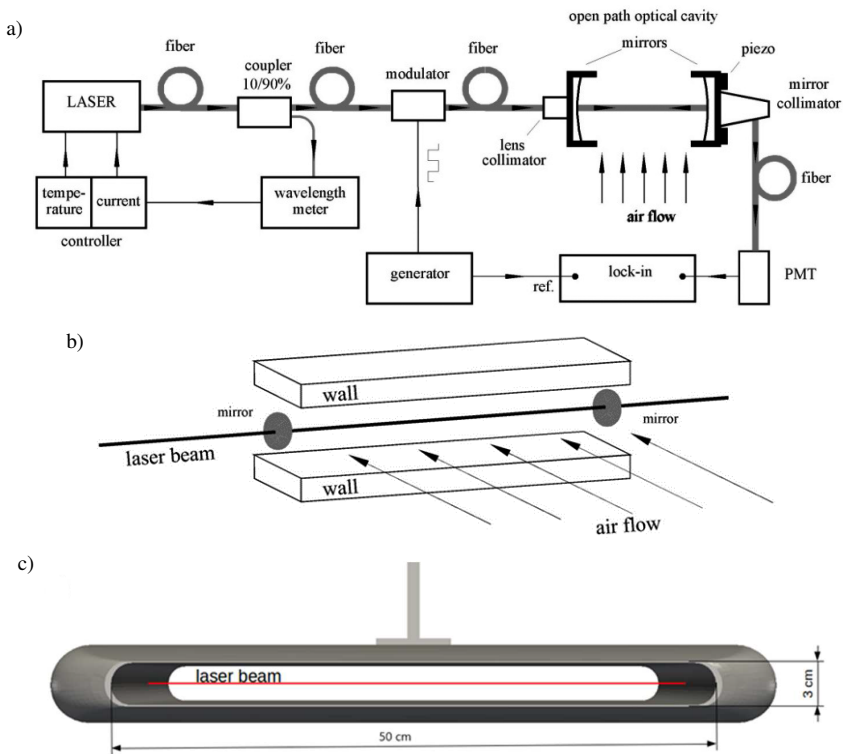

Fig. 6. a) A simplified diagram of the optical hygrometer; b) a scheme of the open-space resonator; c) visualization of the sensor used in numerical simulations of the airflow and water the vapour desorption effect.

The main part of laser radiation was sent from the coupler to the electro-optic modulator. The modulator (Jenoptik, AM 1550) was driven by the digital generator (Tektronix AGF 3102) providing a rectangular wave. The AM square modulation of the optical signal with slopes of about 1 ns was achieved. The modulated light beam was coupled with the optical resonator using the aspheric lens collimator (Thorlabs, F280APC-C). The cavity, 0.5 m long, was built of two concave mirrors (CRD-optics, Inc.). Their reflectivity reached 99.97% while the radius of

curvature was 1 m. That ensured a radiation trapping time $\tau_0 = 5$ μs. The piezoelectric actuator (Thorlabs, PE4) supplied by another sine generator with a frequency of 30 Hz was used for modulation of the cavity length over approximately 1 μm. That ensured variation of cavity mode frequencies causing their periodic matching with the laser radiation. The radiation leaving the cavity was collected in a fibre by the mirror collimator (Thorlabs, RC12SMA) and directed to the infrared photomultiplier (Hamamatsu, H10330A-75). The signal was detected by the lock-in voltmeter (Stanford Research System, SR830). Its reference signal was supplied from the generator driving the electro-optic modulator.

The application of fibre coupling at the resonator input and output enabled the open-space construction of this cavity. Precise matching of cavity radiation to the output fibre collimator, that is necessary for the signal coupling with the photodetector, served also as efficient space filtering. It reduced the light from external sources (see Fig. 6a). The photomultiplier was additionally protected against the external radiation by the resonance interference filter (Thorlabs, FB1400-12). That was sufficient even against direct sunlight illumination of the cavity.

A scheme of the open-space resonator is presented in Fig. 6b. The mirror holders were attached to two walls. The walls (50 cm long, 6 cm wide) were separated by about 3 cm, which means that they were distant about 1.5 cm from the light beam. The airflow between the walls was perpendicular to the laser beam.

The resonator is designed to fit in a typical (PMS type[1]) canister [24]. The optical and electronic elements of the instrument can be arranged in such a way that the hygrometer can be used as a modular sensor in all research aircraft equipped with receptacles for such canisters, operating within a typical range of actual air speeds (50–150 m/s) during the measurements.

3.2. Solving problem of water desorption

Measurement of the atmospheric water vapour density at a level of 10^{12} cm^{-3} and lower should be performed in free air. Otherwise, when the investigation is carried out with an air sample stored in a cuvette or passing through a tube, the result might be affected by H_2O adsorbed/desorbed from the apparatus walls. This is especially important for measurements performed from an aircraft. The hygrometer walls cover with a dense layer of adsorbed H_2O molecules (even 10^{17} cm^{-2}) when the aircraft passes through the lower part of troposphere with a large water content. These molecules are desorbed at higher altitudes (where the water concentration is smaller by several orders of magnitude) and strongly disturb the results [23]. In open-path optical hygrometers the air is just probed with the radiation, without any contact of the investigated sample with the apparatus. Therefore, the result might be free of such interferences [25]. In order to verify the above statement the distortion of the measurement results by desorption of water molecules from the walls of our open-air cavity in the laboratory and the real measurement conditions was studied.

In the first study we estimated desorption in simplified simulations of laboratory climate chamber measurements. In a laminar flow of 0.6 m/s through the cavity the trajectory of a water molecule starting from the upper or the bottom wall of the resonator and going towards the laser beam region was studied by solving the diffusion equation. We found that the probability that the molecule reaches the resonator centre is below 10^{-20} for any atmospheric pressure considered.

In the second study we performed *Direct Numerical Simulations* (DNSs) of the flow around and through the aerodynamically shaped sensor cavity (Fig. 6c) during airborne measurements.

---

[1]PMS canister is in the form of a cylinder with semispherical closures. The canister length is about 800 mm and its diameter is about 177.8 mm.

The calculations were performed for middle and upper troposphere (80 m/s true air speed at pressure of 500 hPa and 150 m/s true air speed at pressure of 300 hPa, respectively) for pitch angles of 0 and 2 degrees. We used *OpenFOAM* software [*openfoam.org*]. A computational mesh, prepared using *snappyHexMesh* tool, composed primarily of hexahedra, had cells small enough (ca. 2 mm) to resolve the scales of the atmospheric turbulence characteristic for middle and upper troposphere. Thus, the robust *icoFoam* solver for laminar flows (DNS) could be used.

Figure 7 presents an example of the simulation results. In Fig. 7a the airflow at 150 m/s true air speed at 300 hPa pressure and 2° pitch angle is presented. Transparency enables to visualize flow disturbances in the whole modelled volume. It can be seen, that there are no significant eddies or circulations, which could influence the measurement along the beam path. In the other simulations disturbances of the flow were even smaller; there is no sign of turbulence or re-circulations inside the cavity. This is confirmed by Fig. 7b where the concentration of passive scalar (the medium that is not influencing the flow – *i.e.* H_2O molecules) is released from the instrument surface at a rate of 0.02 m/s in the central plane of the cavity. The scalar is immediately blown, due to the high speed of flowing air. The simulation results confirm that that water desorption should be not a problem for the presented sensor design.
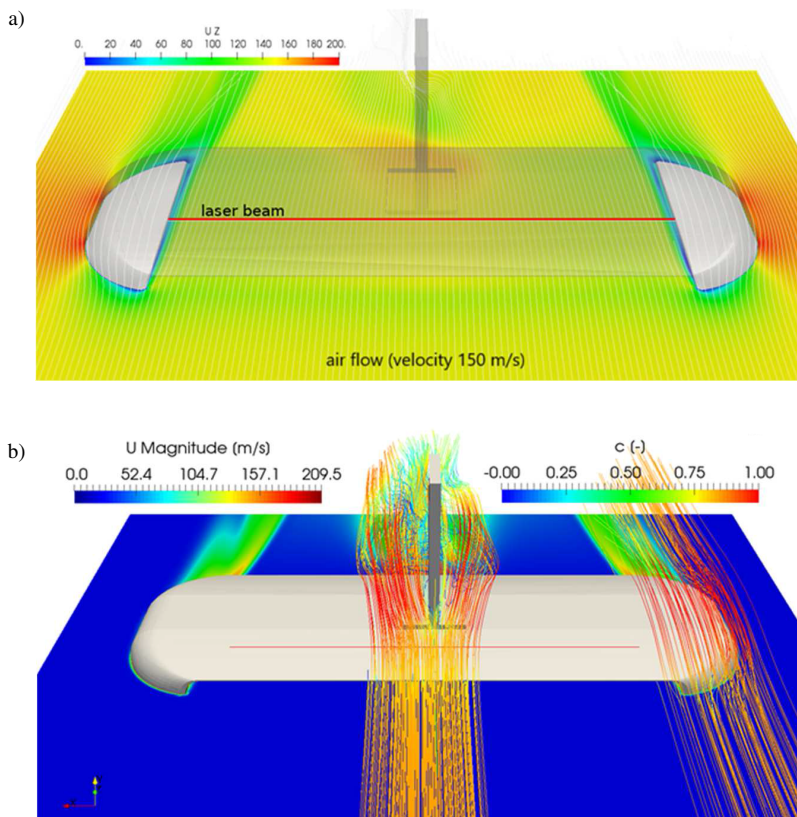

Fig. 7. Selected results of numerical simulations of airflow through the instrument: a flow velocity through the cavity at 150 m/s true air speed and 2° pitch angle of the instrument; transparency enables to visualize all regions with velocity perturbations (a). A flow velocity along selected streamlines (left colour scale) and the central plane concentration of a passive scalar released (concentration $c = 1$, release rate 0.02 m/s) from the surface of the sensor (right colour scale) (b).

3.3. Cavity adjustment

The experiment was started with cavity adjustment. To ensure access to the screws regulating the mirror position in gimbals, this procedure was performed in open air on an optical table. In order to reduce the laser beam absorption by atmospheric water the cavity was filled with gaseous N_2 evaporated from the Devar vessel with liquid nitrogen. The flow rate of nitrogen was about 1 l/min. To minimize the absorption by residual H_2O vapour the laser was tuned to the wavelength of 1391.3092 nm corresponding to the minimal absorption cross-section (Fig. 2). A Proper cavity adjustment was possible in such conditions. We achieved the phase shift value $\varphi_0 = 0.6$ rad at a modulation frequency of 20 kHz. That corresponds to the photon lifetime in the cavity of about $\tau_0 = 5.6 \ \mu s$ and the mirror reflectivity $R = 0.9997$.

3.4. Laboratory tests

In order to check the capability of water vapour determination at low atmospheric pressures (at high altitudes) the system was installed in a vacuum chamber evacuated by an oil-free scroll pump (Anest Iwata ISP-250C) to the ultimate pressure of $3 \cdot 10^{-5}$ atm. The H_2O content was additionally regulated by a freezer with liquid nitrogen. The test was performed with the laser light tuned to the line with the peak at 1392.5335 nm. The measurement of hygrometer linearity (Fig. 8) was started just after the pump was switched off. In that case the chamber was being slowly filled up with laboratory air (humidity of about 25% at 21°C) and with the gas desorbed from the walls.
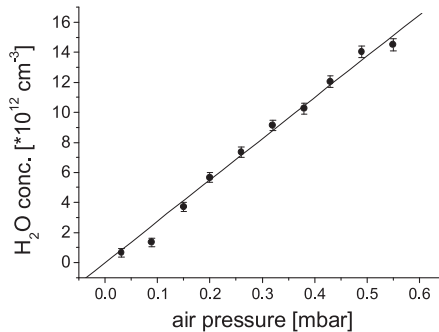

Fig. 8. Linearity of the optical hygrometer.

The minimal H_2O concentration that was registered in our system was $8.6 \cdot 10^{11}$ cm^{-3} at the residual air pressure of $3 \cdot 10^{-5}$ atm in the chamber. The signal average time was about 60 s. In this measurement the experimental error raised with H_2O concentration from 3% at $1.5 \cdot 10^{13}$ cm^{-3} to about 42% at the lowest values.

A shape of the 1392.5335 nm line registered in these conditions is presented in Fig. 9. The continuous line corresponds to the theoretical shape of Doppler broadened absorption line that should occur in such conditions. A large scattering of the experimental points results from a limited stability of wavelength control and from the pure signal-to-noise level at such a low H_2O concentration, so the approximated reproduction of the line profile was very poor. These uncertainties cause even negative values of the absorption coefficient in some cases.

The uncertainty of the measurement (evaluated from the experimental results) was about 16%, which corresponds to the error of $\pm 1.4 \cdot 10^{11}$ cm^{-3}. The error can be also evaluated due to
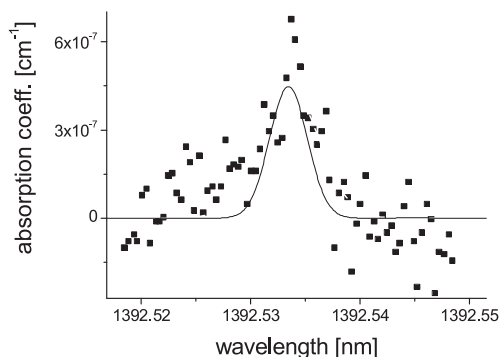
Fig. 9. The line 1392.5335 nm registered at the H_2O concentration of $8.6 \cdot 10^{11}$ cm^{-3}.

the differentiation of (3). It gives the formula for the hygrometer sensitivity limit:

$$N_G = \frac{2\pi n f}{\sigma c \sin^2 \varphi_{n0}} \Delta\varphi_n. \tag{5}$$

Our experiment was performed with the first harmonic ($n = 1$), and we reached the value $\varphi_{10} = 0.6$ rad. The precision of the phase measurement was $\Delta\varphi_1 = 0.006$ rad for the integration time of 30 s. In vacuum the cross-section is about $\sigma = 5.58 \cdot 10^{-19}$ cm^2 (Fig. 3a), then the detection limit is about $N_G = 1.4 \cdot 10^{11}$ cm^{-3}, which is consistent with the previous evaluation. That corresponds to the mean water vapour concentration at altitudes above 40 km (Fig. 1). In normal conditions (1000 hPa) the cross-section drops to a value of about $4.8 \cdot 10^{-20}$ cm^2, then the sensitivity of the system also decreases to $N_G = 1.6 \cdot 10^{12}$ cm^{-3}.

4. Discussion and conclusion

The recent progress in optoelectronics opens a capability to construct fully optical sensors of water vapour in various gases. As far as in these constructions the gas is tested with a light beam, the measurement takes place practically without disturbance. Our experiment shows that a CRDS open-path optical hygrometer working in the 1392–1393 nm spectral range may be one of the most sensitive instruments of this type. The detection limit of our system ($1.4 \cdot 10^{11}$ cm^{-3} at low pressures) was limited by a relatively poor mirror reflectivity: $R = 0.9997$ only. As far as the mirrors with the reflectivity coefficient of 0.99999 are available, the hygrometer might be about ten times more sensitive [25, 26].

There are various other ways of improving the hygrometer construction. First of them consists in using a better wavelength control system which would be rather based on a reference cell with water vapour than on a wave-meter. Using the line of 1392.5335 nm such an instrument can be successfully applied to atmospheric humidity measurements in the upper troposphere and across the stratosphere at altitudes of 5–50 km.

For measurement of larger humidity a weaker absorption line can be applied (Fig. 2) in order to avoid the instrument saturation. Such a saturation can occur when the values of time constant τ used in (1) approach the rise/fall time of a square-modulated input signal. In the spectral band there are lines which peak cross-sections vary within three orders of magnitude (and even much more due to the pressure effect). Therefore, tuning the laser to a properly selected line one can

www.czasopisma.pan.pl   PAN   www.journals.pan.pl
POLSKA AKADEMIA NAUK
T. Stacewicz, P. Magryta, et al.: HIGHLY SENSITIVE AIRBORNE OPEN PATH OPTICAL…

ensure precise work of the hygrometer within all water vapour concentrations that can occur in atmosphere: from 10^{18} cm^{-3} down to 10^{10} cm^{-3}. Additional opportunities of enlarging the range and precision are in adjusting the modulation frequency and in selection of an harmonic (3). An aerodynamically shaped open-path cavity design enables undisturbed fast-response measurement of air humidity. Both size and mechanical design of the instrument sensing part enable to construct a hygrometer fitting a PMS-type receptacle for modular instruments, the standard in many modern research aircraft.

Acknowledgments

References

[1] Myhre, G., Shindell, D., Bréon, F.M., Collins, W., Fuglestvedt, J., Huang, J., Koch, D., Lamarque, J.F., Lee, D., Mendoza, B., Nakajima, T., Robock, A., Stephens, G.N., Takemura T., Zhang, H. (2013). *Anthropogenic and Natural Radiative Forcing. Climate Change 2013: The Physical Science Basis. Contribution of Working Group I to the Fifth Assessment Report of the Intergovernmental Panel on Climate Change*. Cambridge, United Kingdom and New York, NY, USA: Cambridge University Press.

[2] Dessler, A.E., Schoeber, M.R., Wang, T., Davis S.M., Rosenlof, K.H. (2013). Stratospheric water vapor feedback. *PNAS*, 110(45), 18087–18091.

[3] Hegglin, M.I., Plummer, D.A., Shepherd, T.G., Scinocca, J.F., Anderson, J., Froidevaux, L., Funke, B., Hurst, D., Rozanov, A., Urban, J., von Clarmann, T., Walker, K.A., Wang, H.J., Tegtmeier S., Weigel, V. (2014). Vertical structure of stratospheric water vapour trends derived from merged satellite data. *Nature Geoscience*, 7(3), 768–776.

[4] Kärcher, B., Dörnbrack, A., Sölch, I. (2014). Supersaturation Variability and Cirrus Ice Crystal Size Distributions. *J. Atmos. Sci.*, 71(3), 2905–2926.

[5] Jensen, E.J., Diskin, G., Lawson, R.P., Lance, S., Bui, T.P., Hlavka, D., McGill, M., Pfister, L., Toon, O.B., Gaog, R. (2013). Ice nucleation and dehydration in the Tropical Tropopause Layer. *PNAS*, 110(6), 2041–2046.

[6] Dyroff, C., Sanati, S., Christner, E., Zahn, A., Balzer, M., Bouquet, H., McManus, J.B., González-Ramos, Y., Schneider, M. (2015). Airborne in situ vertical profiling of HDO/H$_2^{16}$O in the subtropical troposphere during the MUSICA remote sensing validation campaign. *Atmos. Meas. Tech.*, 8(4), 2037–2049.

[7] Hurst, D.F., Read, W.G., Vömel, H., Selkirk, H.B., Rosenlof, K.H., Davis, S.M., Hall, E.G., Jordan, A.F., Oltmans, S.J. (2016). Recent divergences in stratospheric water vapor measurements by frost point hygrometers and the Aura Microwave Limb Sounder. *Atmos. Meas. Tech.*, 9(9), 4447–4457.

[8] Rothman, L.S., Gordon, I.E., Babikov, Y., Barbe, A., Chris Benner, D., Bernath, P.F., Birk, M, Bizzocchi, L., Boudon, V., Brown, L.R., Campargue, A., Chance, K., Cohen, E.A., Coudert, L.H., Devi, V.M.; Drouin, B.J., Fayt, A., Flaud, J.M., Gamache, R.R., Harrison, J.J., Hartmann, J.M., Hill, C., Hodges, J.T., Jacquemart, D., Jolly, A., Lamouroux, J., Le Roy, R.J., Li, G., Long, D.A., Lyulin, O.M., Mackie, C.J., Massie, S.T., Mikhailenko, S., Müller, H.S.P., Naumenko, O.V., Nikitin, A.V., Orphal, J., Perevalov, V., Perrin, A., Polovtseva, E.R., Richard, C., Smith, M.A.H., Starikova, E., Sung, K., Tashkun, S., Tennyson, J., Toon, G.C., Tyuterev, V.G., Wagner, G. (2013). The HITRAN 2012 molecular spectroscopic database. *Journal of Quantitative Spectroscopy and Radiative Transfer*, 130(1), 4–50.

[9] Bange, J., Esposito, M., Lenschow, D.H., Brown, P.R.A., Dreiling, V., Giez, A., Mahrt, L., Mali-nowski, S.P., Rodi, A.R., Shaw, R.A., Siebert, H., Smit, H., Zöger, M. (2013). *Measurement of Air-craft State and Thermodynamic and Dynamic Variables, in Airborne Measurements for Environmen-tal Research: Methods and Instruments* (eds. Wendisch, M., Brenguier, J.L.), Weinheim, Germany: Wiley-VCH Verlag GmbH & Co. KGaA.

[10] Foken, T., Falke, H. (2012). Technical Note: Calibration device for the krypton hygrometer KH20. *Atmos. Meas. Tech.*, 5(3), 1861–1867.

[11] Elliott, W.P., Gaffen, D.J. (1991). On the utility of radiosonde humidity archives for climate studies. *Bull. Am. Meteorol. Soc.*, 72(10), 1507–1520.

[12] Zondlo, M.A., Paige, M.E., Massick, S.M., Silver, J.A. (2010). Vertical cavity laser hygrometer for the National Science Foundation Gulfstream-V aircraft. *J. Geophys. Res.*, 115, D20309.

[13] Buchholz, B., Böse, N., Ebert, V. (2014). Absolute validation of a diode laser hygrometer via inter-comparison with the German national primary water vapor standard. *Appl. Phys. B.*, 116(3), 883–899.

[14] Buchholz, B., Ebert, V. (2018). Absolute, pressure-dependent validation of a calibration-free, airborne laser hygrometer transfer standard (SEALDH-II) from 5 to 1200?ppmv using a metrological humidity generator. *Atmos. Meas. Tech.*, 11(1), 459–471.

[15] Sonnenfroh, D.M., Kessler, W.J., Magill, J.C., Upschulte, B.L., Allen, M.G., Barrick, J.D.W. (1998). In-situ sensing of tropospheric water vapor using an airborne near-IR diode laser hygrometer. *Appl. Phys. B*, 67, 275–282.

[16] Nowak, J.L., Magryta, P., Stacewicz, T., Kumala, W., Malinowski, S.P. (2016). Fast optoelectronic sensor of H$_2$O concentration. *Optica Applicata*, 46(3), 607–618.

[17] Abe, H., Yamada, K.M.T. (2011). Performance evaluation of a trace-moisture analyzer based on cav-ity ring-down spectroscopy: Direct comparison with the NMIJ trace-moisture standard. *Sensors and Actuators A: Physical*, 165(2), 230–238.

[18] O'Keefe, A., Deacon, D.A.G. (1988). Cavity ring-down optical spectrometer for absorption measure-ments using pulsed laser sources, *Rev. Sci. Instrum.*, 59(12), 2544–2551.

[19] Berden, G., Engel, R. (2010). *Cavity Ring-Down Spectroscopy: Techniques and Applications*. Wiley-Blackwell.

[20] Herbelin, J.M., McKay, J.A., Kwok, M.A., Uenten, R.H., Urevig, D.S., Spencer, D.J., Benard, D.J. (1980). Sensitive measurement of photon lifetime and true reflectance in an optical cavity by a phase-shift method, *Appl. Opt.*, 19, 144–147.

[21] Lisak, D., Hodges, J.T., Ciuryło, R. (2006). Comparison of semiclassical line-shape models to rovi-brational H$_2$O spectra measured by frequency-stabilized cavity ring-down spectroscopy. *Phys. Rev. A*, 73(1), 012507–012513.

[22] Hodges, J.T., Lisak, D., Lavrentieva, N., Bykov, A., Sinitsa, L., Tennyson, J., Barber, R.J., Tolchenov, R.N. (2008). Comparison between theoretical calculations and high-resolution measurements of pres-sure broadening for near-infrared water spectra. *J. Mol. Spectrosc.*, 249(2), 86–94.

[23] Sedlak, P., Sikula, J., Majzner, J., Vrnat, M., Fitl, P., Kopecky, D., Vyslouzil, F., Handel, P.H. (2012). Adsorption-desorption noise in QCM gas sensors. *Sensors and Actuators B: Chemical*, 166–177, 264–268.

[24] Norment, H.G. (1988). *Three-Dimensional Trajectory Analysis of Two Drop Sizing instruments: PMS OAP and PMS FSSP. NASA Contractor Report 4113*, DOT/FAAjCT-87130, National Aeronautics and Space Administration, USA.

[25] May, R.D. (1998). Open-path near-IR tunable diode laser spectrometer for atmospheric measurements of H$_2$O. *J. Geophys Res.*, 103(D15), 19161–19172.

[26] Abe, H., Kitano, H. (2011). Improvement of flow and pressure controls in diffusion-tube humidity generator: Performance evaluation of trace-moisture generation using cavity ring-down spectroscopy. *Sensors and Actuators A: Physical*, 136(2), 723–729.